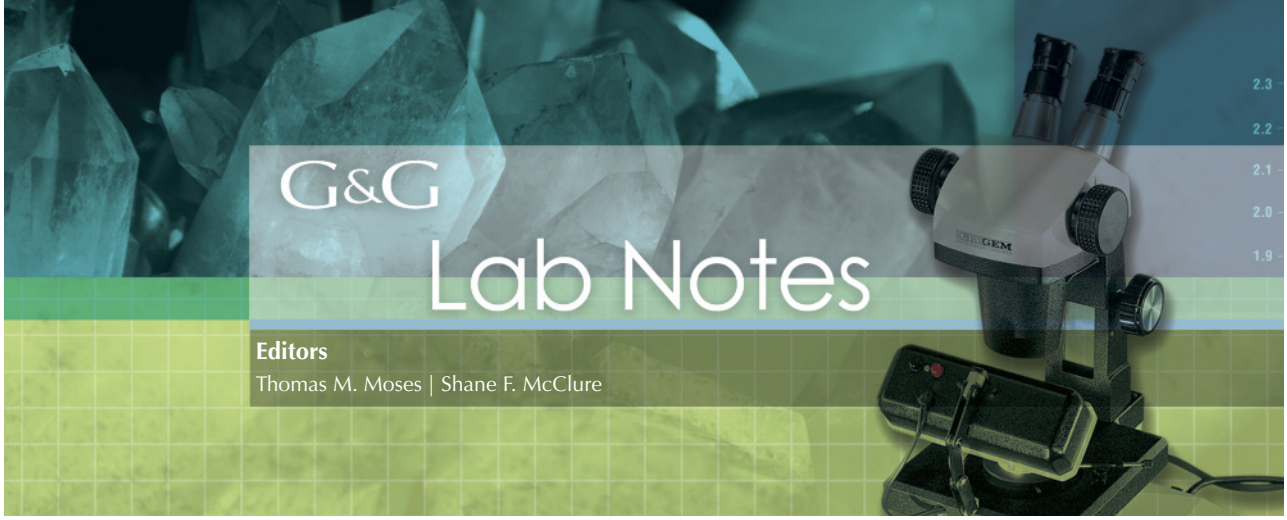

DIAMOND

Black, with Unusual Color Origin

A 1.75 ct Fancy black round brilliant diamond (figure 1) was submitted to the Carlsbad laboratory for color origin determination. Natural black diamonds are usually colored by inclusions of sulfides, graphite or other mineral inclusions or, in rare cases, hydrogen-related clouds that extend throughout the stone. Treated black diamonds are generally heavily fractured stones that are subjected to high-temperature, low-pressure treatment, which graphitizes the fractures, turning them black. Artificial irradiation can also produce a dark enough color so as to appear black, but this is less common (H. Kitawaki, "Gem diamonds: Causes and colors," *New Diamond and Frontier Carbon Technology*, Vol. 17, No. 3, 2007, pp. 119–126).

Upon initial examination, the stone was noted to be covered in large, deeply penetrating fractures; therefore, high-pressure, low-temperature treatment was suspected. Yet closer examination revealed that the fractures were surrounded by dark brown radiation stains. Patches of non-fractured surface on the pavilion showed the normal transparency of diamond, causing the radiation staining to stand out in relief. Because radiation stains in diamond are inert to short-wave ultraviolet light, we placed the stone in a DTC DiamondView to confirm their identity. Figure 2 shows numerous fractures surrounded by dark bands, which are the radiation stains.

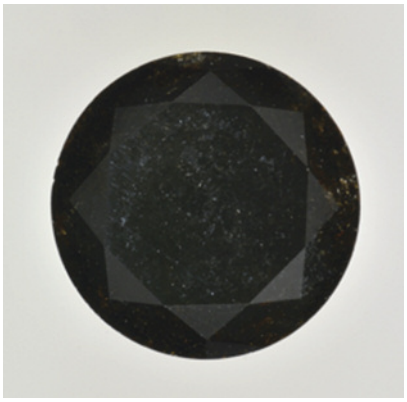

Figure 1. A face-up view of the 1.75 ct black diamond.

Natural radiation stains provide an important clue to the color origin of a diamond. Diamonds that have been naturally colored by radiation can have stains associated with that color, though this is not a definitive criterion. In this case, the stains are so numerous and thick that they cause the diamond color. A close-up view of the pavilion (figure 3) shows the relative transparency of the diamond contrasted with the highly saturated color of the radiation staining of the fractures. The coverage of the stains is so complete that only a few transparent areas can be seen in the face-up view. Some of the color was due to the presence of small black inclusions, but most was due solely to the natural radiation stains, an unusual cause of color.

Troy Ardon

Figure 2. A DiamondView image showing the pattern of inert radiation stains following the fractures in the stone.

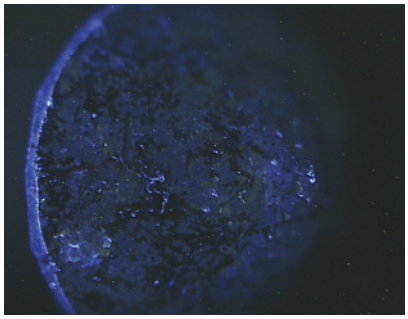

Figure 3. This image of the pavilion shows the patchwork nature of the radiation staining. Magnified 55×.

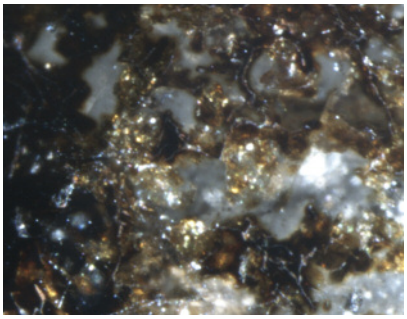

Silicon in Natural Type IIa and Type IaB

The presence of Si in diamond is typically revealed by detection of the

Editors' note: All items were written by staff members of GIA laboratories.

GEMS & GEMOLOGY, Vol. 49, No. 4, pp. 252–256, http://dx.doi.org/10.5741/GEMS.49.4.252.

© 2013 Gemological Institute of America

736.6/736.9 nm ("737 nm") doublet zero-phonon line (ZPL), observed by either absorption or photoluminescence (PL) spectroscopy. This feature has been assigned to the negatively charged state of the silicon split-vacancy defect, SiV^-, which is frequently incorporated into CVD synthetic diamonds due to the etching of silicon-containing growth chamber components. Conversely, reports of the 737 nm peak in natural or HPHT synthetic diamonds are notably rare (see C.M. Breeding and W. Wang, "Occurrence of the Si-V defect center in natural colorless gem diamonds," *Diamond and Related Materials*, Vol. 17, 2008, pp. 1335–1344; Winter 2010 Lab Notes, p. 302; Winter 2012 Lab Notes, pp. 304–305). Consequently, this feature is considered an important tool for identifying CVD synthetic diamonds.

Recently, SiV^- was detected in the PL spectra (liquid-nitrogen temperature with 633 nm laser excitation) of five diamonds submitted to GIA's Mumbai laboratory. These 0.31–0.90 ct round brilliants were issued colorless grades of either D or E. Their clarity grades ranged from VVS_1 to SI_2, where the lower grades arose from the presence of trapped crystalline inclusions.

FTIR spectroscopy revealed that four of the samples were type Ia, with hydrogen-related peaks at 3107 and 1405 cm^{-1}. The remaining sample was type IIa, with no discernible impurity-related IR features. Multi-laser, liquid-nitrogen-cooled PL spectra acquired for the fifth sample were similar to those reported in Breeding and Wang's 2008 investigation of SiV^- in natural diamonds. The latter also showed luminescence at 737, 714.6, 589.8, 557.8/558.2, 554.2, and 550.3 nm, in addition to $NV^{0/-}$ (575 and 637 nm, respectively) and 3H (503.4 nm). This SI_2 sample contained several inclusions with intact crystalline faces, identified by Raman spectroscopy as olivine, consistent with the former investigation (figure 4, top). Through gemological and spectroscopic observations, it was possible to distinguish this natural type IIa diamond from Si-containing type IIa CVD synthetics.

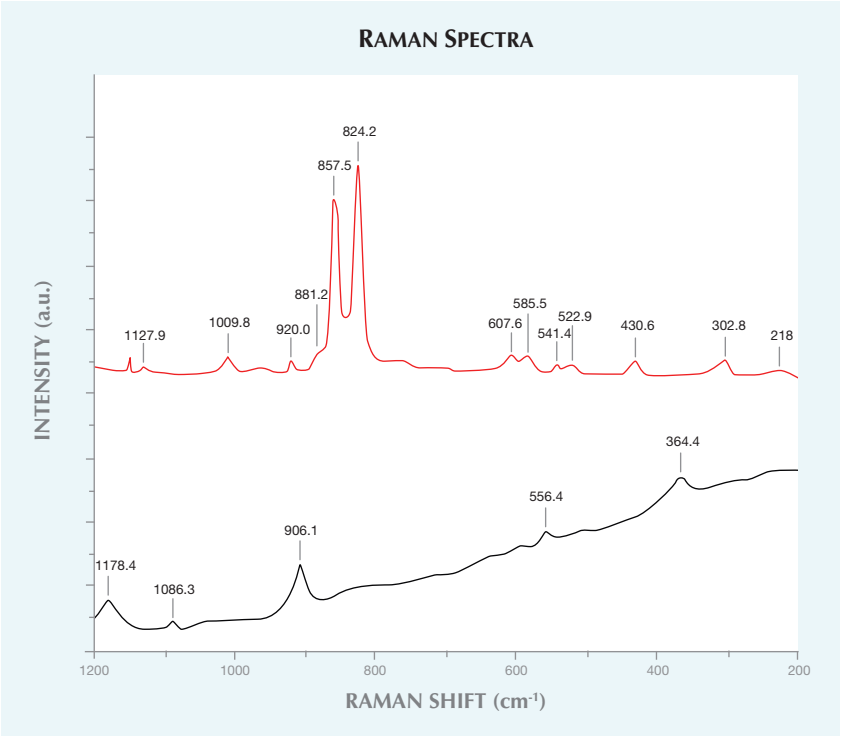

Figure 4. Room-temperature Raman spectroscopy (830 nm laser excitation) identified the different inclusions in the type IIa, SI_2 (top) and type IaB, SI_1 (bottom) natural diamonds containing silicon. The former spectrum is consistent with olivine, while the latter is attributed to spessartine garnet.

The type Ia diamonds studied by Breeding and Wang all contained A-aggregates and varying concentrations of B-aggregates (type IaA±B). In the present group of type Ia diamonds, only B-aggregates were detected (pure type IaB). With the exception of the 737 nm feature, the type IaB diamonds' PL spectra did not include any of the spectroscopic features characteristic of Si-containing type IaA±B diamonds. An emission line at 664.3 nm was detected in all the type IaB specimens, however. These samples also showed emissions from $NV^{0/-}$ (575 and 637 nm, respectively), H3 (503.2 nm), and H4 (495.9 nm), where H4 was remarkably strong for three of the diamonds. Interestingly, the diamond with the lowest H4 concentration was also distinctly included (SI_1 clarity). Raman spectroscopy identified the inclusions as spessartine garnet (figure 4, bottom). Breeding and Wang also reported the presence of garnet in Si-containing diamonds. The presence of olivine and garnet inclusions in natural diamonds containing SiV^- has been suggested to indicate that they crystallized in an area of mixed-composition peridotite in the upper mantle.

These results emphasize that the detection of SiV^- in diamonds does not unequivocally signify CVD synthetic origin. Nevertheless, careful analysis of spectroscopic features and crystalline inclusions can be used to separate these natural diamonds and their synthetic counterparts.

Ulrika F. S. D'Haenens-Johansson, Manisha Bhoir, and Kyaw Soe Moe

Stellate Zircon Inclusions in Vivid Purple-Pink MORGANITE

The Carlsbad laboratory recently examined a 4.95 ct vivid purple-pink morganite. In addition to its saturated color, the stone was particularly noteworthy because of the inclusions it contained. Microscopic examination revealed numerous stellate inclusions, each with many delicate tapered legs (figure 5).

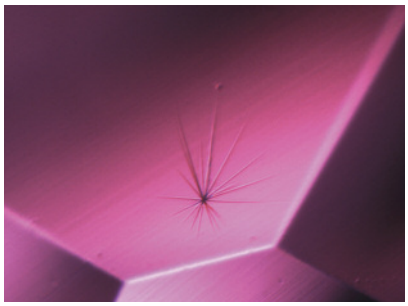

Figure 5. Stellate clusters of zircon needles were observed in this purple-pink morganite. Vertical field of view 0.58 mm.

Gemological properties revealed an RI of 1.577–1.583 and a hydrostatic SG of 2.73. It did not show fluorescence under either long- or short-wave UV. All of these properties were consistent with beryl, which was further confirmed by FTIR and Raman spectroscopy.

Figure 6. The needle-like zircons showed a sub-adamantine luster when examined using reflected light. The largest surface-breaking needle measures approximately 10 microns in the longest cross-sectional direction.

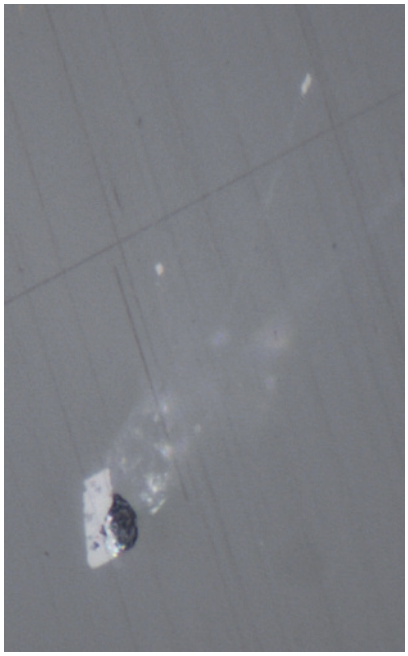

Inclusions in the stone showed an interesting starburst pattern, with thin needles radiating from a central point of nucleation. Viewed with polarized light, the needles exhibited birefringence. A sub-adamantine luster was observed where some of the needles broke the surface (figure 6). Raman spectroscopy identified the inclusions as zircon, consistent with our initial observations. Zircon inclusions are occasionally found in pegmatitic beryl, but they usually occur as prismatic or rounded crystals that cause damage to their host due to zircon's relative instability (E.J. Gübelin and J.I. Koivula, *Photoatlas of Inclusions in Gemstones*, ABC Edition, Zurich, 1986, p. 197).

In addition to the zircon clusters, the stone also contained fluid inclusions, transparent crystals, particulate clouds, and singular needles. The distinctive morphology of the zircon inclusions, coupled with the vivid purple-pink color, create a rather unique gemstone.

Tara Allen and Nathan Renfro

SPINEL Submitted as Diamond

Diamond simulants remain in wide circulation and are a common sight in the GIA laboratory. Even so, it is rare that we encounter a natural gemstone masquerading as a colored diamond. The New York laboratory recently received a 0.50 ct rough sample with a remarkably saturated Fancy Intense

Figure 7. This rough spinel, submitted as a diamond, displayed trigons oriented in the direction opposite that of the crystal face.

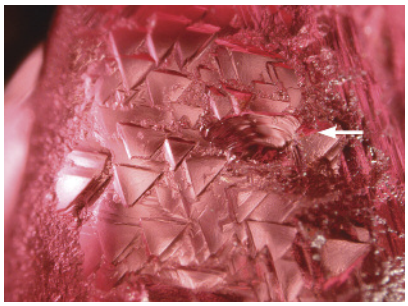

Figure 8. In addition to trigons, the spinel displayed a conchoidal fracture (see arrow), a feature not found in diamond. Magnified 40×.

to Vivid pink color (figure 7) for a Colored Diamond Identification and Origin Report. The stone displayed octahedral crystal form with numerous trigons on its crystal faces. These triangular etch pits, caused by chemical dissolution, are common characteristics of both natural diamond and spinel but have also been observed in flux synthetic spinels (M.S. Krzemnicki, "Trade Alert: Flux grown synthetic red spinels again on the market," *SSEF Newsletter*, October 14, 2008, p. 3). When found on octahedrons, trigons point in the direction opposite that of the crystal face, as in figure 7. Figure 8 shows a distinctive conchoidal fracture amid the trigons, a feature alien to diamond. This feature, along with the sample's striking color, indicated something other than diamond.

The high-resolution UV-Vis spectrum displayed emission bands and absorption peaks not seen in natural diamond. Closer examination of the photoluminescence spectrum affirmed chromium peaks at 685, 687, 689, and 700 nm. Chromium causes the red/pink color in spinel but is not present in diamond. The narrow bandwidth of the 685 nm peak, along with the presence of the ~533 nm band in the UV-Vis spectrum, proved this was an untreated stone (S. Saeseaw et al., "Distinguishing heated spinels from unheated natural spinels and from synthetic spinels: A short review of ongoing research," www.giathai.net/pdf/Heated_spinel_Identification_at_May_

25_2009.pdf). Other observations included a specific gravity of 3.45–3.48, consistent with spinel, as well as medium to strong red long-wave and short-wave UV. Though submitted for a diamond report, this stone was actually a natural pink spinel.

This finding serves as a reminder of the importance of both standard gemological techniques and advanced spectroscopy in identifying gem materials.

Martha Altobelli, Paul Johnson, and Kyaw Soe Moe

Large SYNTHETIC MOISSANITE with Silicon Carbide Polytypes

Silicon carbide (SiC) is composed of a carbon atom surrounded by four silicon atoms in a tetrahedral form. Colorless synthetic moissanite is pure silicon carbide; the incorporation of impurities produces colors, including black. Its high hardness (second only to diamond) and thermal conductivity make it a convincing diamond simulant. Both transparent and opaque synthetic moissanites have been submitted to GIA's laboratory over the past two decades. In this report, we examine a 29.73 ct synthetic moissanite submitted as a black diamond (figure 9, left).

An uneven surface and surface-breaking black inclusions were visible with the unaided eye. Mosaic patterns of light and dark gray regions were observed under a microscope and became distinct in the Raman image (figure 9, right). Small cavities and polish lines in different directions were present on the table surface, and a granular texture was observed in a large cavity on the girdle. Raman spectroscopy identified the dark gray regions as silicon carbide.

Interestingly, each random testing spot showed mixed bands of silicon carbide polytypes (i.e., identical chemical composition but a slightly different crystal structure). The polytype 6H-SiC (6 = the number of stacking sequences, H = hexagonal, and SiC = silicon carbide) was detected by Raman bands at 789.6, 765.0, and 148.0 cm^{-1}. Other polytypes were also distinguished by Raman bands: 3C-SiC (C = cubic) at 970.1, 968.4, 797.8, 795.4, and 788.2, cm^{-1}; 4H-SiC at 785.7 cm^{-1}; and 15R-SiC (R = rhombohedral) at 768.4 cm^{-1} (figure 10; see also P. Colomban, "SiC, from amorphous to nanosized materials, the example of

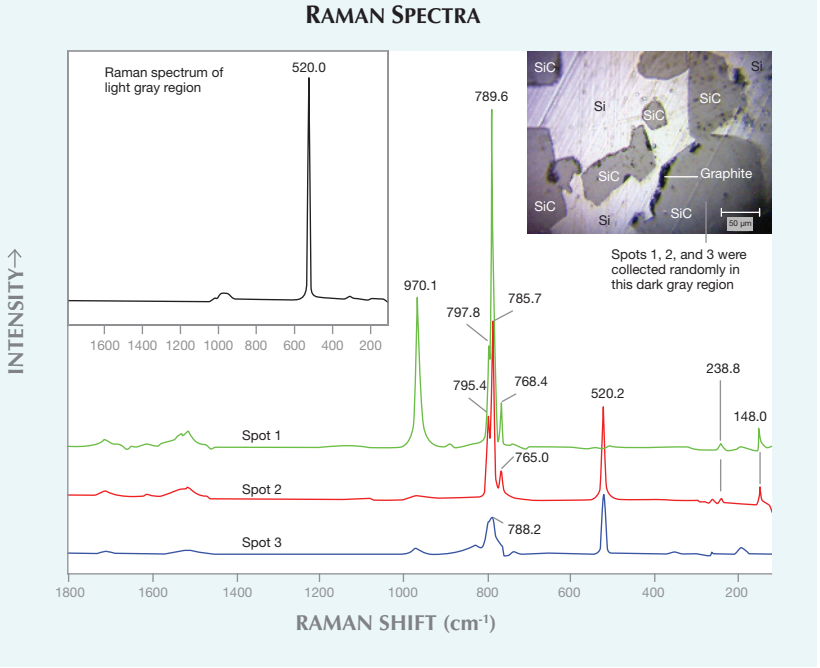

Figure 10. Each random spot showed mixed Raman bands of silicon carbide polytypes: 6H-SiC at 789.6, 765.0, and 148.0 cm^{-1}; 3C-SiC at 970.1, 968.4, 797.8, 795.4, and 788.2 cm^{-1}; 4H-SiC at 785.7 cm^{-1}; and 15R-SiC at 768.4 cm^{-1}. Silicon was also found at 520.2 cm^{-1} in spots 2 and 3. Bands at 238.8 cm^{-1} (possibly related to 6H-SiC) and 148.0 cm^{-1} (6H-SiC) were missing at spot 3. Light gray regions with a band at 520.0 cm^{-1} (left inset) were identified as silicon; the black regions were identified as graphite. The spectra have been shifted vertically for clarity.

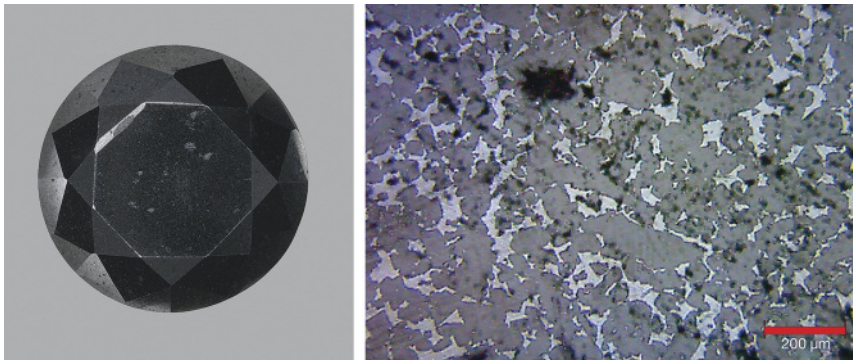

Figure 9. This 29.73 ct synthetic moissanite (left) was submitted as a black diamond. Surface-breaking graphite inclusions were easily observed, including the largest one at the upper left table edge. The mosaic patterns on the table surface became distinct when viewed under a Raman microscope (right).

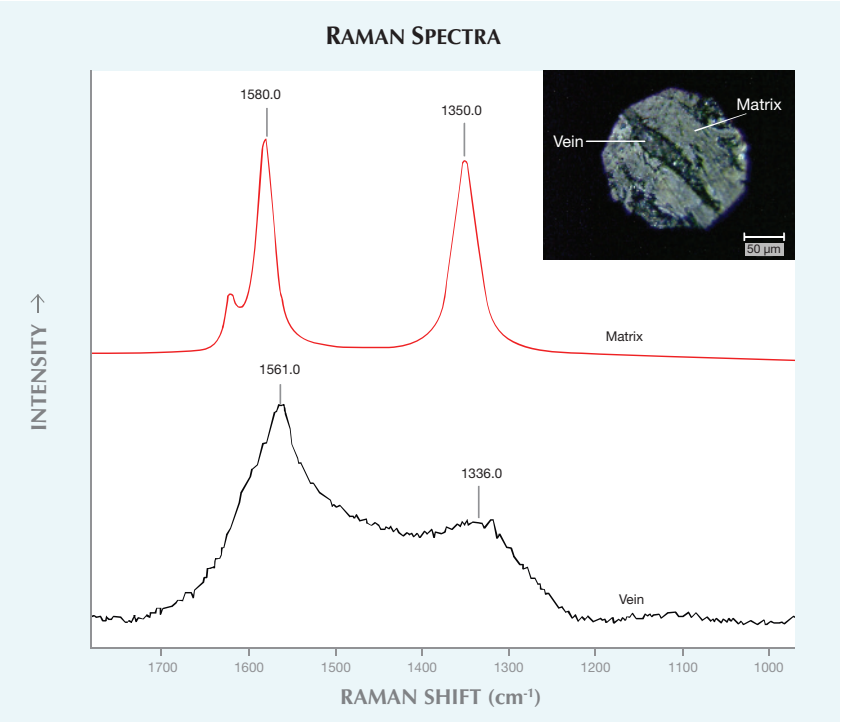

Figure 11. Micro-imaging of a graphite inclusion (inset) showed a vein in matrix. The matrix was composed of crystalline graphite, as suggested by sharp Raman bands at 1580.0 and 1350.0 cm^{-1}. The vein was identified as amorphous graphite by broad bands at approximately 1561.0 and 1336.0 cm^{-1}.

SiC fibers issued of polymer precursors," in M. Mukherjee, Ed., *Silicon Carbide—Materials, Processing and Applications in Electronic Devices*, InTech, 2011, pp. 161–186). In addition to these bands, a sharp Raman band assigned to silicon was detected at 520.2 cm^{-1} at a few spots. Bands corresponding to 6H-SiC at 238.8 and 148.0 cm^{-1} could not be detected at all measurement locations. Light gray regions were identified as silicon at 520.0 cm^{-1} (figure 10, left inset). Black inclusions, both eye-visible and microscopic, were confirmed as graphite. As figure 11 illustrates, the micro-image of a graphite inclusion showed an amorphous graphite vein (broad Raman bands at approximately 1561.0 and 1339.0 cm^{-1}) inside a crystalline graphite matrix (sharp bands at 1580.0 and 1350.0 cm^{-1}).

During SiC growth, rotation along the covalent bond generated alternate stacking layers of Si and C atoms along the c-axis with different structural sequence, which is noticeable in the $(11\bar{2}0)$ plane but not along the basal plane. This rotation can occur at very low energy. Since constant growth energy is difficult to control, two or more silicon carbide polytypes can form simultaneously during the growth process; this phenomenon is called *polytypism*. Raman spectroscopy has been used to detect these polytypes. Although there are more than 250 known polytypes, SiC can be classified as either beta (β) or alpha (α) type. The beta type crystallizes in cubic lattice symmetry (e.g., 3C-SiC), the alpha type in hexagonal symmetry (e.g., 6H-SiC).

Traditional growth methods for silicon carbide involve sintering and hot pressing, and there are also newer techniques. Reaction-bonded silicon carbide can form when liquid silicon reacts with porous graphite. This silicon carbide contains both pure silicon (as a bonding component), and graphite. Earlier studies have suggested that black synthetic moissanite containing silicon inclusions could be grown by the physical vapor transport (PVT) method (see Winter 2009 GNI, p. 308; Spring 2011 Lab Notes, pp. 54–55). Using PVT, researchers have grown large silicon carbide bulk crystals up to 50 × 25 mm at a rate of 1.2 mm per hour at 10 kPa pressure (Q.–S. Chen et al., "Growth of silicon carbide bulk crystals by physical vapor transport method and modeling efforts in the process optimization," *Journal of Crystal Growth*, Vol. 292, 2006, pp. 197–200). Nevertheless, Raman analysis at several testing points confirmed only the 6H-SiC polytype.

This sample was submitted for a Colored Diamond Identification and Origin Report, but one should always pay close attention to surface features, such as the mosaic pattern of light and dark gray regions in reflected light, together with surface-breaking black inclusions not observable in black diamond.

Kyaw Soe Moe, Paul Johnson, and Ren Lu

PHOTO CREDITS:
Robison McMurtry—1; Troy Ardon—2 and 3; Nathan Renfro—5 and 6; Joshua Balduf—7; Martha Altobelli—8; Sood Oil (Judy) Chia—9 (left); Kyaw Soe Moe—9 (right), 10 (right inset), and 11 (inset).